John F. O'Hanlon K. C. Park A. Reisman R. Havreluk J. G. Cahill

Electrical and Optical Characteristics of Evaporable-Glass-Dielectric AC Gas Display Panels

Abstract: This paper presents the characteristics of a prototype gas display panel fabricated with electron-beam deposited dielectric films. It is shown that panels with a 6- μ m-thick dielectric layer and a 0.2- μ m-thick MgO layer exhibit short stabilization times (15 min), long life (20 000 h), small drift effects (<0.5 V), and adequate brightness (21 cd/m²). The devices have a large dynamic write margin (>10 V) over a wide pressure range. Dielectric glass layers as thin as 3.2 μ m were found to be stable. A panel with a small H₂O impurity concentration was used to show that the hydrated MgO surface caused charge leakage and loss of memory margin, while a panel with an air leak confirmed that the surface saturated before the effects of gas contamination were observed.

Introduction

This paper describes the electrical and optical characteristics of ac gas display panels fabricated by a newly developed vacuum deposition process. The display panel parts were fabricated on soda-lime glass substrates using metallurgy and dielectric layers deposited from electron-beam heated sources, after which the panel parts were sealed, viscous flow cleaned, and filled with Ne-0.1% Ar in a furnace of controlled ambient gas. Using this process, panels have been produced with stable electrical characteristics, long lifetimes (>20 000 h), and large static memory margins (18 V).

This paper focuses on the electrical and optical characteristics of prototype gas panel display structures which were fabricated with electron-beam deposited borosilicate glass dielectric layers 6 μ m thick, overcoated with 0.2 μ m of MgO, and filled with Ne-0.1% Ar in the pressure range 4 × 10⁴ to 5.3 × 10⁴ Pa (300 to 400 torr). Most structures were sealed in a dry air ambient, but some were sealed in Ne-0.1% Ar or in N₂. The properties of a few devices were studied over a wider pressure range— 2 × 10⁴ to 8 × 10⁴ Pa (150 to 650 torr). Panels similar to this prototype structure, but with various borosilicate glass dielectric thicknesses (2.0 to 11.0 μ m) were studied to determine their current brightness relationships and long-term stability. Also included are characterizations of

two panels, one of which had an air leak and a second which was intentionally doped with H_2O . Studies of device modeling as well as detailed descriptions of the metallurgy, dielectric deposition, and the single-cycle sealing and filling furnace are treated in accompanying papers [1-4]. The seal glass has been described elsewhere [5].

Experimental techniques

• Structure

The static electrical data reported here were taken on small gas display panels fabricated from two 0.64-cm-thick \times 6.4-cm \times 10.5-cm soda-lime glass substrates. The area enclosed by the seal glass was approximately 4.5 cm \times 4.5 cm; the chamber spacing was 0.01 cm. The active cell area consisted of an array of 23 \times 23 cells on 5.08 \times 10⁻²-cm centers. The back plate metallurgy consisted of 0.01-cm-wide horizontal lines. "Tuning-fork" lines, that is, two 0.005-cm-wide lines spaced 0.005 cm apart and running in a vertical direction, constituted the front plate metallurgy. Alternate lines were accessed from opposite sides of the substrate as depicted in Fig. 1.

Dynamic operating data were taken on a larger gas display panel structure consisting of a 6 by 10 array of 240 characters; each character contained a 7×9 array of cells

Copyright 1978 by International Business Machines Corporation. Copying is permitted without payment of royalty provided that (1) each reproduction is done without alteration and (2) the *Journal* reference and IBM copyright notice are included on the first page. The title and abstract may be used without further permission in computer-based and other information-service systems. Permission to *republish* other excerpts should be obtained from the Editor.

613

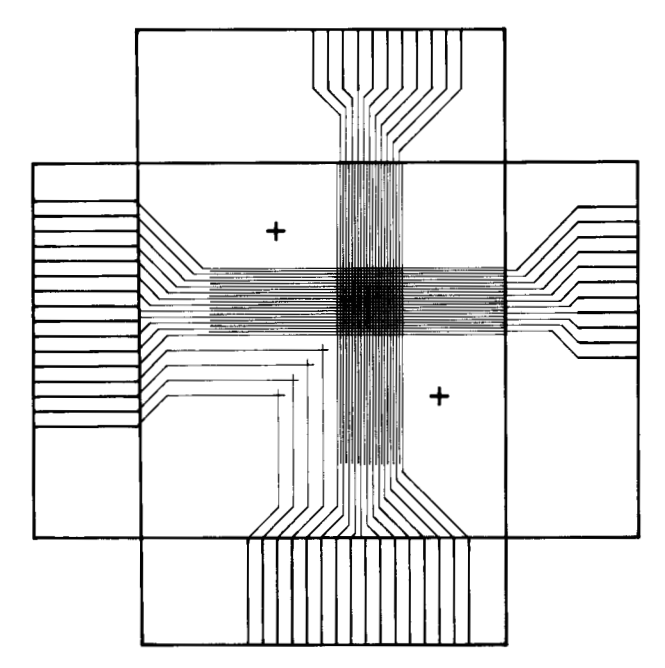


Figure 1 Geometry of the gas display panel. The device contains a 23×23 array on 0.05-cm centers, plus four individual cells.

identical to those employed in the panel illustrated in Fig. 1. All panels were filled with Ne-0.1% Ar following a conventional vacuum bake or the single-cycle sealing and viscous cleaning process [4].

• Electrical measurements

For purposes of measuring the static maximum sustain, \bar{V}_s , and the static minimum sustain, \underline{V}_s , voltages, the panels were operated with a 30-kHz square wave voltage with a rise time of \leq 180 ns. See Fig. 2(a). In all cases, the time to peak avalanche current was 400 to 800 ns, so that the voltage was fully switched before the light pulse was emitted.

To measure the static \bar{V}_s and \bar{V}_s , a square wave voltage of sufficient magnitude was applied between the horizontal and vertical (tuning fork) electrodes such that the entire panel was ignited. The voltage was then reduced to a value that caused one set of alternate, or interdigitated, lines, say, the even numbered lines, to remain extinguished when their electrical connection, shown in Fig. 2(b), was momentarily interrupted. Beginning with that initial condition, two measurements were made: The maximum sustain voltage of the even numbered lines was measured by increasing the voltage to the onset of ignition, and then, after re-establishing this initial condition, the minimum sustain voltage of the odd numbered lines was measured by reducing the sustain voltage to the point at which the odd numbered lines began to be extinguished. After these voltages $\bar{V}_{s}^{\text{even}}$ and $\underline{V}_{s}^{\text{odd}}$ were recorded, the complementary initial condition was established, and in a similar manner, \bar{V}_s^{odd} and $\underline{V}_s^{\text{even}}$ were measured. The static sustain panel margin was then defined as the difference between the highest \underline{V}_s and the lowest \bar{V}_s . Two kinds of static \bar{V}_s and \underline{V}_s data were taken: first cell on/off and twelfth cell on/off. A difference of more than a volt between the two measurements usually implied some form of local defect. For example, particulate matter on the oxide surface or an irregularity in the linewidth caused the operating voltages for a particular cell to be shifted from those of the remainder of the cells. First-cell data were used for quality control; the twelfth-cell data reported here were more representative of the basic device parameters.

Many of the panels fabricated during the course of this study were subjected to a particular test called the "alternate-line-aging" test. During this test panels were operated at midpoint sustain voltage, $\underline{V}_{\rm s}$ + 1/2 $V_{\rm margin}$. However, the voltage supply to one set of horizontal lines, say, the odd numbered lines, was first removed and then restored. This caused those cells to be extinguished. Panels tested with this initial condition were observed for voltage differences between operated and un-operated cells due to differences in the surface caused either by cleaning of the oxide surface under the operated region or by an accumulation of surface impurities over the unexcited sites.

Although data taken by this static test were of no use in determining write or erase pulse amplitudes, they were of considerable significance in monitoring the initial drift, stability, lifetime, and certain kinds of gas or surface contamination. Experimentally, it was also found that panels with large static memory margins (>10 V) also exhibited large dynamic write margins. For these reasons the majority of the data presented in this paper are static \bar{V}_s and \underline{V}_s . Dynamic data were taken on a few panels to determine the sensitivity of the write pulse amplitude margin to perturbations in chamber spacing and pressure.

• Optical measurements

Optical data were recorded with the photon counting apparatus described in Fig. 3. The display panel was synchronized to the counting apparatus by means of the 1-MHz clock located in the counter. To examine the temporal behavior of the argon afterglow, the width of the gating pulse was set to 200 ns and manually stepped through the time region of interest (0 to 35 μ s).

• Leak testing

During the course of this study it was necessary to develop a technique for measuring leaks in the range 10^{-15} to 10^{-13} Pa-m³/s (10^{-14} to 10^{-12} T-l/s). An accumulation technique was employed in which the test panel was valved

from the system and surrounded by helium at atmospheric pressure. After an accumulation time which varied from 10 min to 16 h, the valve was opened and the collected gas was admitted to the vacuum chamber containing a Uthe Technology Inc., model 300C residual gas analyzer; the helium pressure pulse was read from an oscilloscope. Momentarily before opening the valve, the main valve to the high vacuum pump was throttled to a speed of 2×10^{-3} m³/s. It was calculated that the smallest leak flux detectable, 10^{-15} Pa-m³/s (10^{-14} T-l/s), caused a pressure rise of approximately 1.5×10^{-5} Pa in the valved-off volume of 5×10^{-3} m³ in a time of 16 hours; when the valve was opened the gas pressure pulse in the chamber was calculated to be 1.5×10^{-8} Pa (10^{-10} torr). This test proved satisfactory for detecting the smallest leaks of interest in the fabrication of gas display panels.

Results and discussion

• Characteristics of the prototype design

The electrical properties of evaporable-glass MgO-overcoated display panels were found to exhibit a strong dependence on the nature of the sealing ambient. Both dry air and inert sealing ambients were studied; dry air sealing was used for most of the processing because the electrical properties were superior to those of panels processed with inert gas sealing. Nitrogen gas boil-off from the liquid was used for the seal ambient with no purification, while the Ne-Ar mixture was purified in a liquid nitrogen trap and in two successive heated beds packed with vacuum-fired niobium at 300°C and titanium at 870°C, respectively. The oxidizing atmosphere, research-grade dry air, was not treated in any way. In this section electrical, optical, and material properties of the prototype design are presented. The 6- μ m oxide thickness was chosen so that the gas display panel properly loaded existing driver circuitry.

Initial operation

Panels tested in this laboratory were initially operated at 120 V, a potential in excess of \bar{V}_s , until such time as their operating voltages stabilized. Figure 4 illustrates the static operating voltages during this "burn-in" operation for panels sealed in inert and oxidizing atmospheres; in both cases the burn-in time was short, although the airfired panels stabilized more quickly than did inert-gasfired panels. The initial decrease in operating voltages was due to the removal of contaminants from the gas and active surface, which were subsequently deposited on unoperated surfaces [6, 7]. Emission spectroscopy was used to monitor the clean-up of H_2 and N_2 . The maximum sustain voltage and the memory margin were greater in the air-fired panels than in those fired in nitrogen or neonargon mixtures. Chou [8] has used ion-induced (Ne⁺) sec-

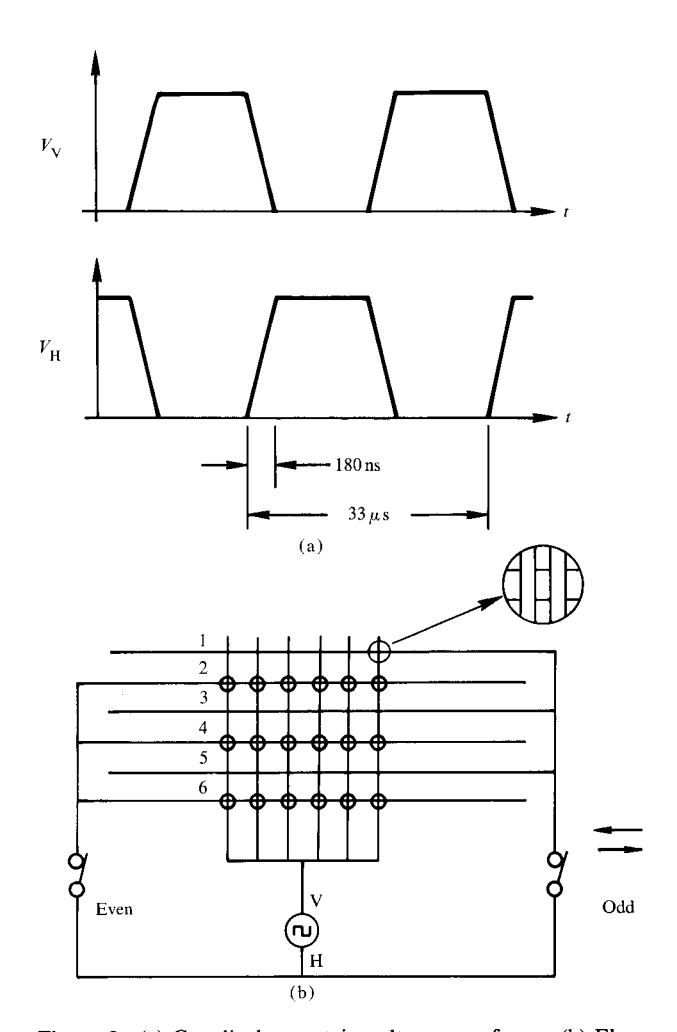
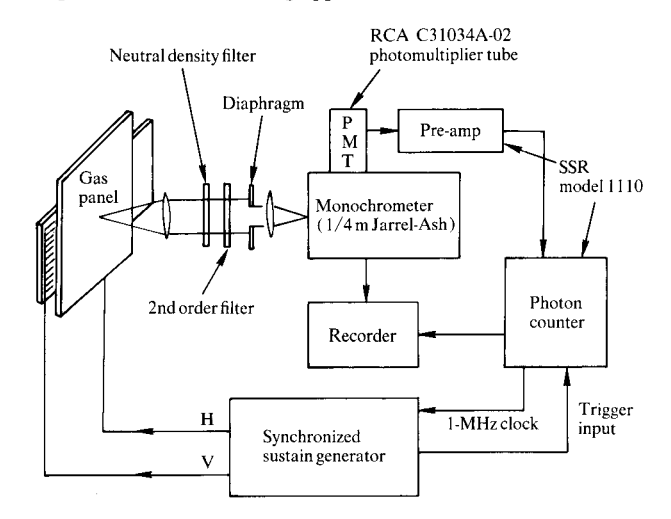


Figure 2 (a) Gas display sustain voltage waveforms. (b) Electrical connection of the gas display panel to excite alternate lines. The excited cells are encircled.

Figure 3 Photon counting apparatus.



615

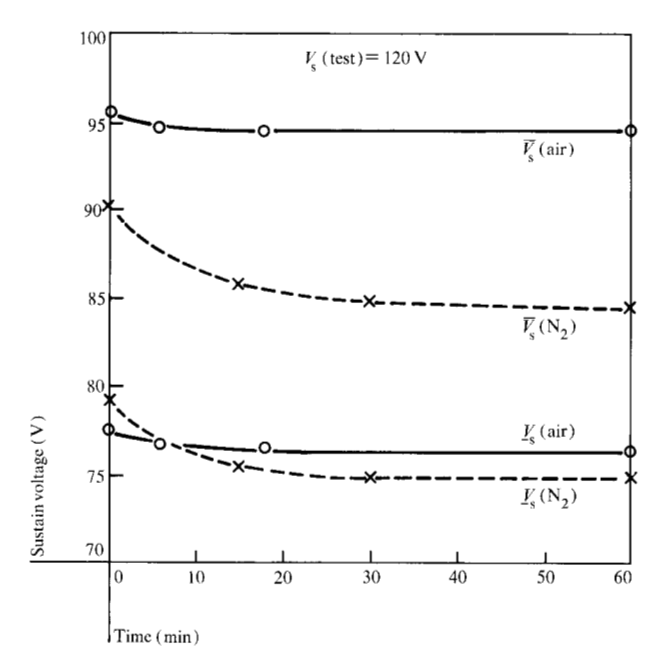


Figure 4 Initial transient behavior of the static operating voltages for inert and air-fired gas display panels (6.5 μ m dielectric, 0.2 μ m MgO).

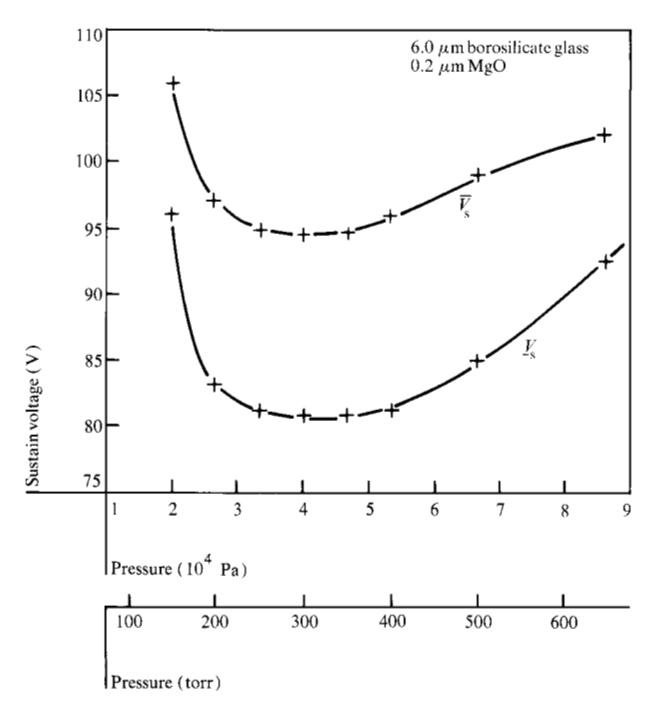


Figure 5 Characteristic Paschen curve of an air-fired gas display panel.

ondary-electron emission to study films of MgO that were subjected to the various sealing environments. He found a secondary-electron yield, γ_i , of 0.45 for electron-spectroscopically clean, as-deposited films, and a yield

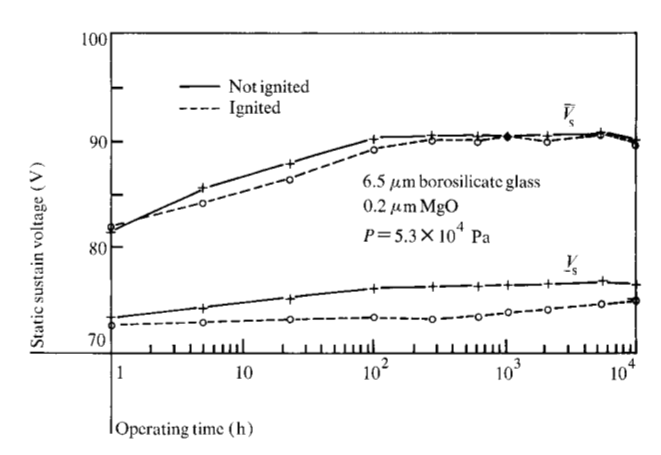


Figure 6 Time dependence of the static sustain voltages for a prototype gas display panel sealed in a nitrogen atmosphere.

 $\gamma_i = 0.27$ for MgO films baked in vacuum at 300°C. He also found $\gamma_i = 0.52$ for MgO films fired in dry air at 500°C [9]. Ahearn and Sahni [7] have argued that excess oxygen produced a large density of acceptor states near the top of the valence band from which Auger electrons of increased energy were emitted, while Sahni and Lanza [10] have theoretically explained that the excess energy of these electrons modified the dependence of γ_i on the reduced electric field at the cathode [11, 12] and thereby increased \bar{V}_s and the margin. Although the use of MgO has been reported elsewhere [6, 13, 14], comparison of the voltage levels was not possible because the linewidth, chamber spacing, gas composition, and pressure, as well as the processing conditions, were not the same.

The prototype devices produced by air firing contained 529 cells, yielded about 31 cd/m², and required a peak avalanche current of 85 mA. The brightness was less (21.2 cd/m²) in larger, 240-character displays where the internal impedance of the driver produced a greater voltage "notch" at the time of avalanche. Characteristics of the static \bar{V}_s and \bar{V}_s for a typical air-fired panel are presented in Fig. 5 for the pressure range 2 × 10⁴ to 8.6 × 10⁴ Pa (150 to 650 torr).

Life testing the prototype structure

Life testing of the prototype display geometry was accomplished by operating the panel at the static midpoint sustain voltage with all lines connected to the driver, but with alternate lines extinguished. Figure 6 depicts the results of operating a panel sealed in nitrogen for 10 000 h. The rise in maximum sustain voltages for both operated and un-operated cells during the first 100 hours was most likely caused by oxygen on the surface of the MgO and was characteristic of panels sealed in this ambient. The severe drift in the minimum sustain voltage exhibited by the un-operated cells was characteristic of panels in which the MgO surface was contaminated [6, 7]. Since no emission spectra of nitrogen, oxygen, or hydrogen appear

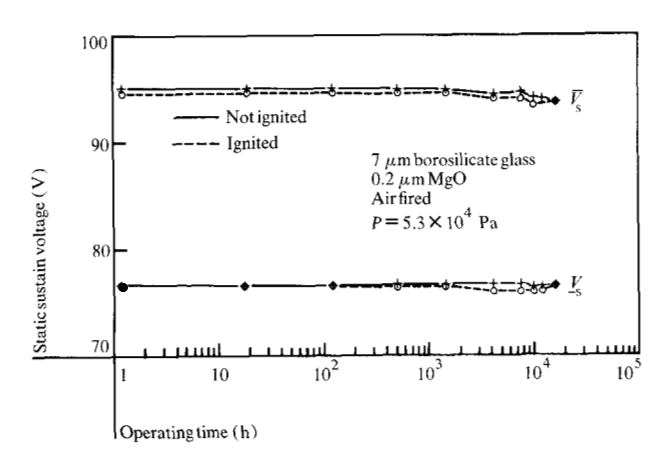


Figure 7 Time dependence of the static sustain voltages for a prototype gas display panel sealed in a dry air atmosphere.

in these panels, and helium mass spectroscopy showed leaks $<10^{-15}$ Pa-m³/s, the impurities located on the surface were either present at the time of filling or diffused to the surface during the initial excitation of the glow discharge.

Figure 7 illustrates the static operating characteristics of a typical, clean, air-fired panel, with a leak rate of less than 10⁻¹⁵ Pa-m³/s. To date the 18-V memory margin has remained stable for 17 000 h. Surface contamination was negligible as no alternate-line-aging greater than 0.5 V was observed.

Dynamic operating data

In an accompanying paper [15], the dependence of the static sustain voltages on pressure and chamber spacing were described. They show that the static margin increased with increased chamber spacing. To complete the characterization of the prototype panel the dynamic write margin was measured on several panels at midpoint sustain voltage. The write margin is $(\tilde{V}_w - V_w)$, where \tilde{V}_w is the maximum write pulse amplitude that can be used without ignition of half-selected cells, and V_{w} is the minimum pulse amplitude that will ignite the cell of interest. Figure 8 depicts the results of dynamic write tests for panels filled to pressures of 5.3×10^4 Pa, 4.8×10^4 Pa, and 4.3×10^4 Pa and having chamber spacings ranging from 0.8×10^{-2} to 1.1×10^{-2} cm. The value of the write margin was large enough, between 10 V and 14.7 V, for proper operation by the driver for all combinations of chamber spacing and pressure tested. However, more extensive measurements may show that the sensitivity to a perturbation in chamber spacing around a value of 10⁻² cm is indeed the least at one pressure.

• Oxide thickness effects

In order to characterize the process in greater detail, panels were fabricated by depositing dielectric layers ranging from $2.0 \mu m$ to $11.0 \mu m$ thick. The dielectric layers were

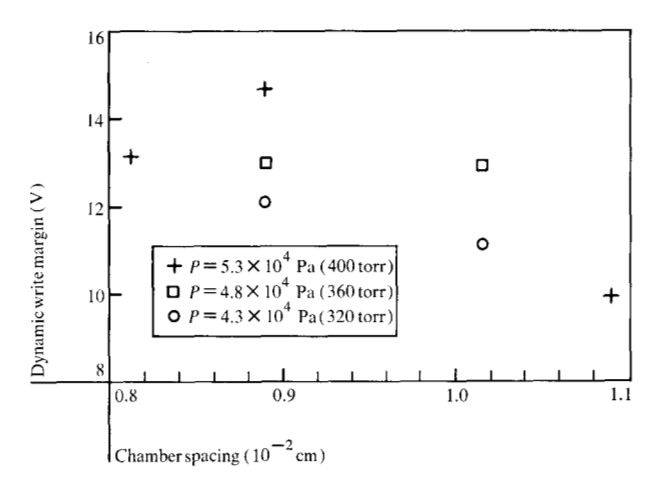


Figure 8 Dynamic write voltage margin dependence on pressure and chamber spacing.

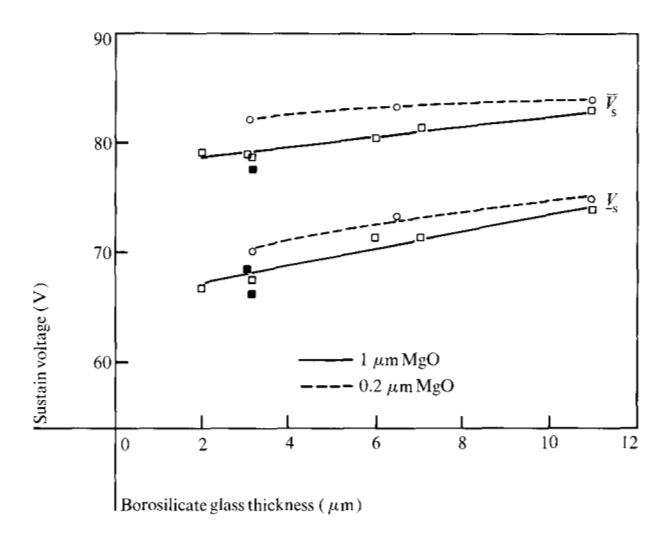


Figure 9 Sustain voltage dependence on dielectric and MgO thicknesses for a 529-cell, inert-gas-fired panel.

overcoated with 0.2 μm to 1.0 μm of MgO. Figure 9 describes the dependence of the static sustain voltages on the dielectric glass thickness for clean, leak-free panels fired in nitrogen or neon-argon mixtures. As the dielectric glass thickness was increased from 2.0 μm to 11.0 μm , the \tilde{V}_s increased from 82 V to 84 V for panels with 0.2 μm MgO, while the sustain margin decreased from 12 V to 9 V. In Figure 10 results are given for a similar set of display panels which were fired in dry air. Here one sees the same behavior as well as the characteristically high \hat{V}_s and large sustain margin.

The change in $\bar{V}_{\rm s}$ with dielectric thickness was attributed to the capacitive voltage divider effect. For a device

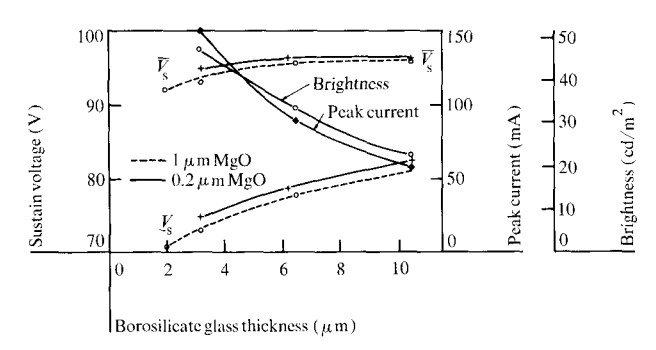


Figure 10 Sustain voltage dependence on dielectric and MgO thickness for a 529-cell air-fired panel.

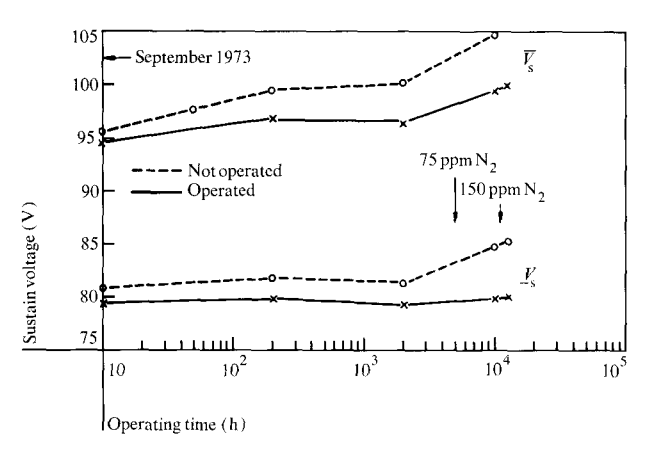


Figure 11 Time dependence of the static sustain voltages for a panel fired in dry nitrogen and containing a 2.6×10^{-13} Pa-m³/s $(2\times10^{-12}$ T-l/s) air leak.

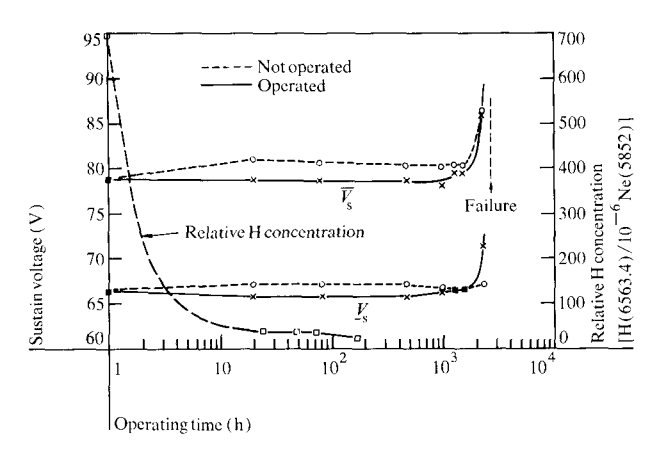


Figure 12 Sustain voltages and relative hydrogen concentration vs time for a panel containing water vapor as an impurity $(P = 4 \times 10^4 \text{ Pa})$.

with no stored charge, the relationship between the applied voltage, $V_{\rm a}$, and the voltage across the gas gap prior to firing, $V_{\rm o}$, can be expressed as

$$\frac{V_{\rm a}}{V_{\rm g}} \; = \; \frac{C_{\rm w} + C_{\rm g}}{C_{\rm w}} \; = \; 1 \; + \; \frac{2t_{\rm d}}{t_{\rm g}\epsilon_{\rm d}} \; + \; \frac{2t_{\rm MgO}}{t_{\rm g}\epsilon_{\rm MgO}} \; , \label{eq:Vg}$$

where $C_{\rm g}$ and $C_{\rm w}$ are the gas and wall capacitances, and $t_{\rm d}$, $t_{\rm g}$, and $t_{\rm MgO}$ are, respectively, the thickness of the dielectric, gas gap, and MgO. The dielectric constants were chosen to be $\epsilon_{\rm d}=4.6$ (see Appendix 1) and $\epsilon_{\rm MgO}=10.8$. Using this expression a 3.2% increase in applied voltage (2.5 to 3.0 V) was calculated for an increase in dielectric thickness from 2.0 μ m to 11 μ m. Experimentally, changes of 2 to 4 V were observed. Increasing the thickness of the MgO yielded quite different results for the two sealing ambients. For the case of panels fired in nitrogen or neonargon, $\bar{V}_{\rm s}$ decreased with increasing MgO thickness. It was postulated that the thicker MgO films had more oxygen vacancies. An insignificant increase in firing voltage, less than 1 V, was observed with thicker MgO when air firing was used.

Brightness and peak current measurements for clean, air-fired panels are depicted in Fig. 10. All of the panels had adequate brightness, $>21 \text{ cd/m}^2$, and with the exception of the 2.0- μ m-thick layers, all had adequate breakdown strength. The desired oxide thickness then becomes a design compromise between the current-carrying capacity and internal impedance of the driver on the one hand and light output on the other.

Life testing of panel structures with dielectric thicknesses of 2.0, 3.3, and 10.5 μ m was also carried out. Devices with 2.0 µm of borosilicate glass failed after 1000 hours of operation. The mode of failure was an increase in both V_s and V_s of over 20 V in a time period of less than 100 hours. Panels with somewhat thicker dielectric layers, 3.3 \(mm\), have accumulated over 20 000 hours of operation to date and have shown only a 2 V increase in sustain voltages. As would be expected, panels fabricated with 10.5 µm of dielectric were found to be stable. The oldest of these panels has been in operation for 11 000 hours. It has less than 0.4 V of alternate-line-aging and only 1 V drift in sustain voltages between 24 hours and 11 000 hours. The minimum thickness for dielectric stability is somewhere between 2.0 and 3.3 μ m, with all panels 3.3 μ m and thicker showing adequate long-term stability.

• Effects of gaseous impurities

The object of this section is to show the effects of two types of impurities, air and water vapor, on the stability and charge storage of MgO-overcoated gas panels. The basic interaction mechanisms of $\rm H_2O, \, N_2, \, \rm CO_2, \, and \, \rm CO_2$ with MgO have been detailed elsewhere [6, 7].

A panel with a known air leak rate of 2.6×10^{-13} Pa-m³/s was operated for 13 000 hours. Analysis of the emission from the 391.4 nm line of nitrogen showed the concentration to be \approx 75 ppm @ 5000 h and 150 ppm @ 11 000 h. The static sustain voltages are given in Fig. 11. Its operating life can be divided into two periods. During the first 2000 hours, the surface was not saturated, while beyond that time the added N_2 , H_2O , O_2 , and CO_2 remained in the gas

phase. In the first time period \underline{V}_s of the operated cells was constant while the remaining voltages increased. Ahearn and Sahni [16] have shown that the inclusion of oxygen in the chamber of an inert-gas-fired panel causes \bar{V}_s of the operated cells to increase, while it has also been shown [7] that the addition of less than 20 ppm of H_2O and O_2 will cause \bar{V}_s and \underline{V}_s of the un-operated cells to increase. Beyond 2000 hours, nitrogen and oxygen cause all cell voltages to increase with time; greater than 20 ppm of N_2 causes the operated cell voltages to increase, while <20 ppm O_2 causes un-operated cell voltages to increase [7].

A second panel was fabricated with a large quantity of H₂O in the gas mixture by filling and effecting tip-off at 463°C, at which temperature there was considerable evolution of H₂O from the glass. The sustain voltages of this panel are depicted in Fig. 12, and the initial results are in agreement with the short-term stability studies of Ahearn and Sahni, that is, V_s and V_s of the operated cells are unchanged while the alternate, un-operated lines show a voltage increase. Emission spectra (H-656.34 nm) taken during the first 168 hours showed the H₂O concentration decreasing to a low level as the surface became saturated with the decomposition products of water vapor. However, this study demonstrated that after 2800 hours of operation, $ar{V}_{\rm s}$ increased sharply until the panel could no longer be operated by the sustain driver. It is postulated that this failure is related to the gross changes in secondary emission of the hydrated surface.

Ahearn and Sahni [17] have observed a strong dependence of the argon afterglow decay rate on impurity level and have measured this rate vs concentration using the dc electrode configuration of an ordinary neon light bulb. Figure 13 presents decay rates measured on four gas panels both clean and with impurities. Because the neon metastables which excite the argon are also lost by diffusion as well, numerical comparison with the bulb geometry is not possible. Curves A and B of Fig. 13 display the decay rates of two clean panels; panel A was fired in dry argon and showed a decay time constant, τ , of 3.1 μ s, while panel B, fired in dry nitrogen, yielded $\tau = 2.7 \,\mu s$. The difference between these two was most likely caused by gas mixture differences. Panel C containing 100 ppm of air had a time constant of 1.9 \mus, while Panel D (H₂O) gave $\tau = 1.0 \mu s$.

Impurities can also be used as probes. Appendix B analyzes the nitrogen afterglow of panel C to show that a plasma exists for some time after the electric field in the gas has decayed.

Analysis of the dependence of the sustain voltages on operating frequency yielded information about the charge retention times of clean and contaminated panels. Voltages \underline{V}_s and \overline{V}_s were measured over the frequency range 100 kHz to 25 Hz, which corresponded to a time interval

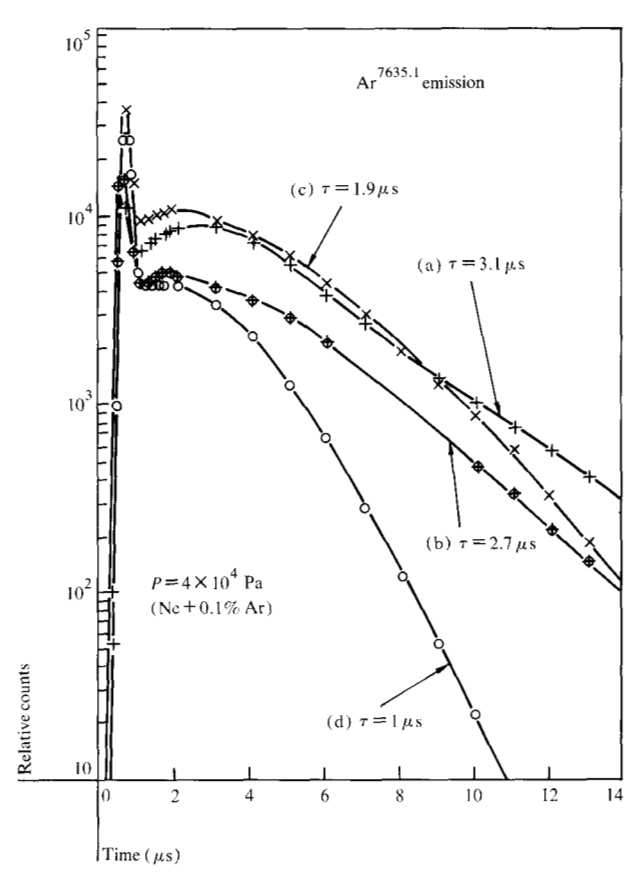


Figure 13 Argon 763.51 nm emission vs panel contamination. (a) Clean, air-fired, (b) clean, N_2 -fired, (c) air leak, 10^{-13} Pa-m³/s, (d) large H_2O impurity.

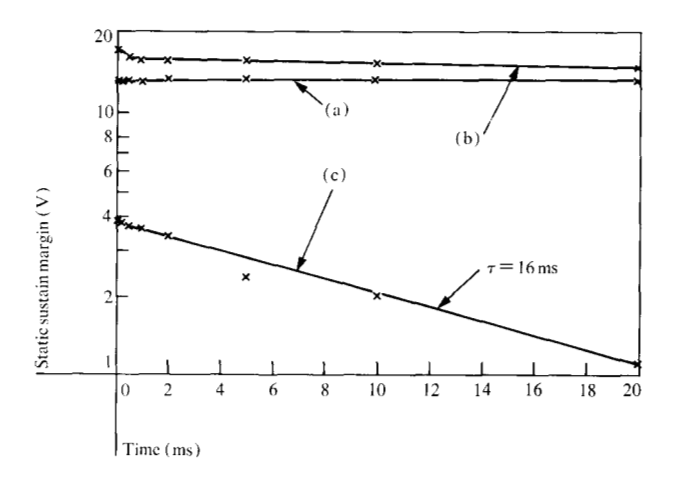


Figure 14 Observed memory margin in three gas display panels vs time interval between firings. (a) Clean, (b) 10^{-13} Pa-m³/s air leak, (c) H₂O impurity.

between successive firings of 5 μ s to 20 ms. Figure 14 displays the static memory margin for three types of panels: clean, air leak, and water-vapor-contaminated. The clean panel showed no loss of memory margin over the fre-

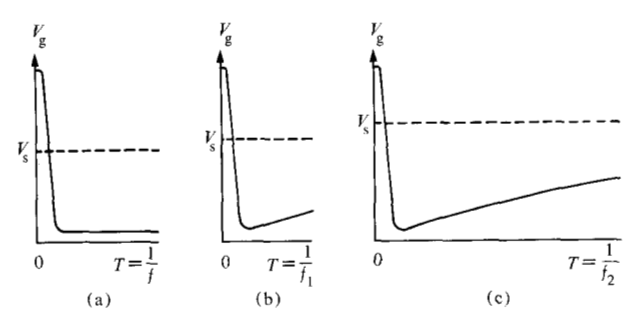


Figure 15 Schematic diagram showing the sustain voltage and gas voltage, V_s , for (a) a clean panel operating at any desired frequency and (b), (c) a panel with charge leakage operated at two frequencies f_1 , f_2 , where $f_1 > f_2$.

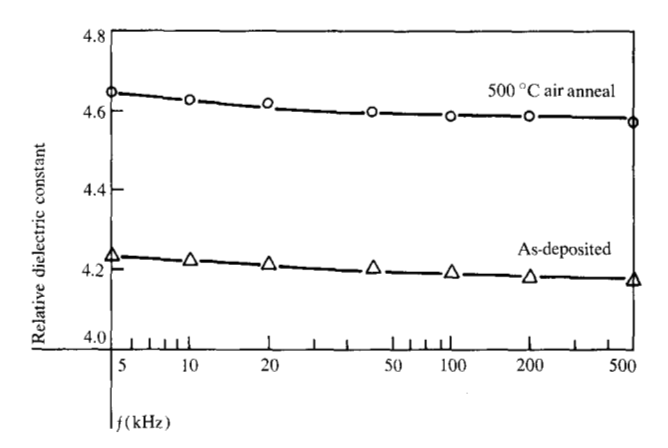


Figure 16 Dielectric constant of $6-\mu m$ borosilicate glass films.

quency range studied. Sahni [18] has found no charge decay for time delays as long as 30 s, by means of electronically interrupting the sustain voltage. Air contamination caused only 2 V degradation in memory margin. However, the water-vapor-doped panel yielded a decay time constant of 16 ms, indicating that the charge stored on the active site was rapidly leaking away. In order for this loss of memory margin to be consistent with the loss of stored charge, \tilde{V}_{s} should increase with lower frequency operation as shown in Fig. 15. Voltage \bar{V}_{c} was observed to increase from 78 V at 100 kHz to 80 V at 25 Hz. This analysis shows that N₂ or O₂ contamination does not degrade charge retention, and postulates that H₂O contamination does produce a charge-leaky hydrated MgO surface. The latter conclusion is in agreement with the findings of Johnson et al. [19].

Summary

This paper has characterized a prototype design of the evaporable-dielectric gas display panel. The design utilized $6.0 \, \mu m$ of electron-beam deposited glass coated

with $0.2~\mu m$ of electron-beam deposited MgO. Clean, leak-free, air-fired panels made with these layers have excellent electrical and optical properties. These panels were shown to have sustain voltages which stabilized quickly (15 min) and remained stable for 17 000 hours; aging effects were less than 0.5 V. It was demonstrated that both the static and dynamic margin were large and stable over a wide pressure range. The measured brightness was greater than $21.2~cd/m^2$ for all sizes of panels constructed for this study.

The properties of panels with other dielectric layer thicknesses and with gas contaminants were also discussed. These studies yielded a minimum, stable dielectric thickness, $3.2~\mu m$, and an understanding of the effects of air and H_2O on the lifetime of MgO-overcoated gas display panels. Panels doped with H_2O can be operated satisfactorily with some alternate-line-aging until such time as the surface no longer resembles MgO. The hydrated MgO surface also destroys the memory margin by allowing stored charge to leak away. A panel with an air leak was used to demonstrate the effects of air contamination on long-term operation. Reactive gases were observed to first saturate the surface and then build up in the gas phase until the panel could no longer be ignited.

Acknowledgment

The authors acknowledge many helpful discussions with O. Sahni and C. Lanza.

Appendix A: The dielectric constant of deposited borosilicate glass films

Borosilicate glass films $6 \mu m$ thick were deposited on platinum coated substrates. Dielectric constant measurements were made on both as-deposited films and films annealed at 500°C in dry air. Aluminum counter electrodes were used after the annealing step was completed. The frequency dependence of the measured dielectric constant is shown in Fig. 16. The values of $\epsilon_{r} = 4.6$ for airannealed films and $\epsilon_r = 4.2$ for as-deposited films contrast with the value of $\epsilon_r = 4.7$ for the bulk source material. The loss factor was found to be $\tan \varphi = 0.006$ for annealed films and 0.005 for as-deposited films over the range of frequencies used (5 kHz to 500 kHz). To investigate densification effects due to annealing, one wafer was scribed and broken into two pieces, after which one half was annealed. Thickness measurements on either side of the break detected no film thickness change within the limit of accuracy of the measurement.

Appendix B: The afterglow plasma

The postulate that a plasma exists after the electric field has decayed was made by Lanza [20], Sahni et al. [1], and Weber [21]. Weber has also proved the existence of the afterglow by means of a complicated electrical measure-

ment of the device capacitance. He demonstrated that the device capacitance changed for as long as 15 μ s after the discharge. This appendix demonstrates the existence of an afterglow for as long as 35 μ s after the discharge by a simple optical technique.

The nitrogen impurity in a previously described panel was used as a probe to monitor the activity in the glow space. The gas panel was operated at a frequency of 12.5 kHz (40 µs half-period) and the nitrogen emission at 391.4 nm and 380.4 nm was sampled by a counter with a 200-ns gate width. Figure 17 displays the results of these measurements. The emission at 391.4 nm from the first negative band resulting from charge transfer between neon ions and nitrogen molecules is only seen during the first $4 \mu s$ after the discharge when the electric field is present. The neon metastables, which sustain the afterglow, also excite the nitrogen and produce emission at 380.4 nm, which is seen for as long as 35 μ s. The decay of these two spectra clearly and simply shows the existence of the afterglow. Measurement times could have been extended beyond 35 μ s by choice of a lower sustain frequency.

References and notes

- 1. W. E. Ahearn and O. Sahni, *IBM J. Res. Develop.* 22, 622 (1978, this issue).
- 2. V. Brusic et al., IBM J. Res. Develop. 22, 647 (1978, this issue).
- K. C. Park and E. J. Weitzman, IBM J. Res. Develop. 22, 607 (1978, this issue).
- A. Reisman, M. Berkenblit, and S. A. Chan, IBM J. Res. Develop. 22, 596 (1978, this issue).
- T. Takamori, A. Reisman, and M. Berkenblit, J. Amer. Ceram. Soc. 59, 312 (1976).
- B. W. Byrum, Jr., IEEE Trans. Electron Devices ED-22, 685 (1975).
- 7. W. E. Ahearn and O. Sahni, 1978 SID International Symposium Digest 9, 44 (1978).
- 8. N. Chou, J. Vac. Sci. Technol. 14, 307 (1977).
- 9. N. Chou, private communication.
- O. Sahni and C. Lanza, Conf. Rec. IEEE-SID Conference Display Devices and Systems, 1976, p. 114.
- 11. O. Sahni and C. Lanza, J. Appl. Phys. 47, 1337 (1976).
- 12. O. Sahni and C. Lanza, J. Appl. Phys. 47, 5107 (1976).
- T. Urade, T. Iemori, N. Nakayama, and I. Morita, Conf. Rec. IEEE-SID Conference Display Devices and Systems, 1974, p. 30.

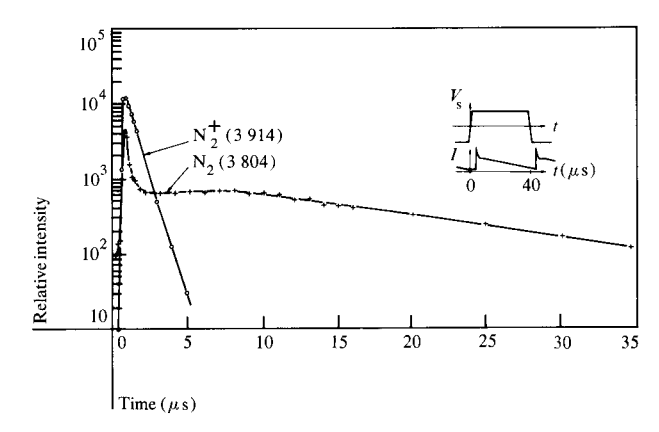


Figure 17 Nitrogen afterglows from a plasma display panel filled to 4×10^4 Pa of Ne-0.1% Ar which was contaminated with 100 ppm of N_2 . The timing of the sustain voltage waveform and the light output are shown in the inset.

- T. Urade, T. Iemori, M. Osawa, N. Nakayama, and I. Morita, IEEE Trans. Electron Devices ED-23, 313 (1976).
- 15. J. F. O'Hanlon, to be published.
- 16. W. E. Ahearn and O. Sahni, private communication.
- 17. W. E. Ahearn and O. Sahni, 27th Annual Gaseous Electronics Conference, Houston, TX, 1974, Abstract IB-6.
- 18. O. Sahni, private communication.
- H. B. Johnson, O. W. Johnson, and I. B. Cutler, J. Amer. Ceram. Soc. 49, 390 (1966).
- 20. C. Lanza, IBM J. Res. Develop. 18, 232 (1974).
- 21. L. F. Weber, Conf. Record IEEE-SID Conference Display Devices and Systems, 1974, p. 20.

Received June 7, 1977; revised January 4, 1978

The authors are located at the IBM Thomas J. Watson Research Center, Yorktown Heights, New York 10598.